Lab on a Chip

Accepted Manuscript

RSC Publishing

www.rsc.org/loc

Registered Charity Number 207890

Graphical Abstract

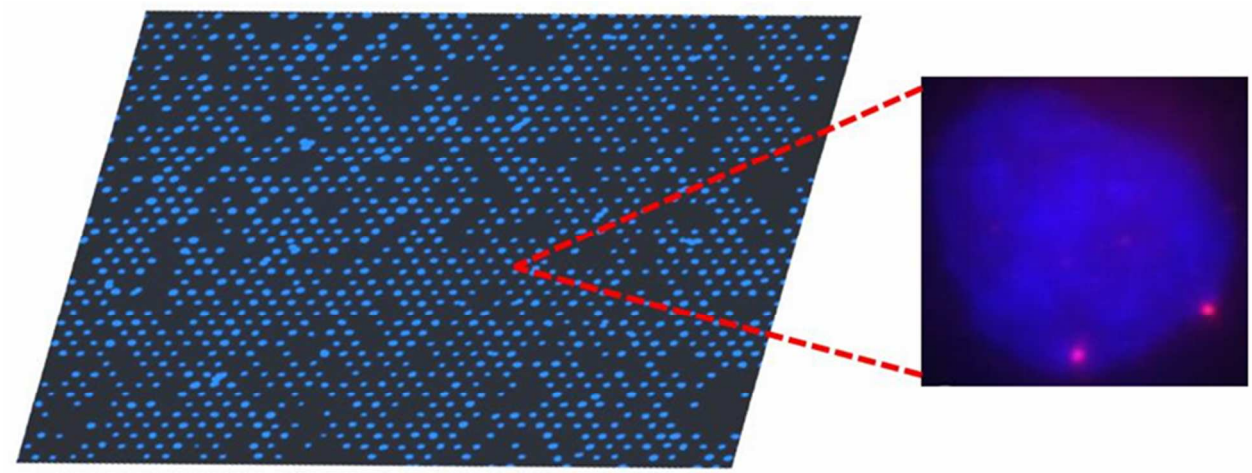

We developed a novel method for generating a centimetre-sized single-cell array, performed DNA fluorescence in situ hybridization (FISH) on the array, and demonstrated feasibility of analyzing the FISH result using a computer program.

Cite this: DOI: 10.1039/c0xx00000x

www.rsc.org/xxxxxx

FULL PAPER

Development of single-cell array for large-scale DNA fluorescence in situ hybridization

Yingru Liu,[a] Brett Kirkland,[a] James Shirley,[b] Zhibin Wang,[a] Peipei Zhang,[a] Jacquelyn Stembridge,[b] Wilson Wong,[c] Shin-ichiro Takebayashi,[b] David M. Gilbert,[b] Steven Lenhert[b,d] and Jingjiao Guan*[a,d]

Received (in XXX, XXX) Xth XXXXXXXXX 20XX, Accepted Xth XXXXXXXXX 20XX
DOI: 10.1039/b000000x

DNA fluorescence in situ hybridization (FISH) is a powerful cytogenetic assay, but conventional sample-preparation methods for FISH do not support large-scale high-throughput data acquisition and analysis, which are potentially useful for several biomedical applications. To address this limitation, we have developed a novel FISH sample-preparation method based on generating a centimetre-sized cell array, in which all cells are precisely positioned and separated from their neighbours. This method is simple and easy and capable of patterning nonadherent human cells. We have successfully performed DNA FISH on the single-cell arrays, which facilitate analysis of FISH results with the FISH-FINDER computer program.

Introduction

DNA fluorescence in situ hybridization (FISH) is a widely used cytogenetic assay that allows assessment of location and copy number of specific DNA sequences in single cells.[1] Conventional FISH is performed on either a thin section of fixed tissues or cells (or cell nuclei) immobilized on a solid surface. The random locations of the cells/nuclei in these samples, and existence of clumped, overlapped, and truncated nuclei, preclude fast and accurate FISH data acquisition and analysis.[2–4] As a result, small numbers (typically less than 100 but occasionally up to 2000) of nuclei are examined in a conventional FISH assay.[5–7] On the other hand, the ability to perform FISH on large numbers of cells could permit accurate quantification and/or sensitive detection of intercellular genetic heterogeneity. Examples include quantifying spatial distribution of genetic elements in nuclei,[6,7] detecting rare circulating cells with cancer-causing genetic mutations, and quantifying intratumor genetic heterogeneity that may be responsible for drug resistance and relapse of cancers.[8,9] A promising approach to realizing such large-scale FISH is to arrange a large population of suspended cells into a two-dimensional array, in which all cells are precisely positioned, isolated from their neighbours, and organized at a high density. This array-based format would, in principle, allow automated, high-throughput data acquisition and analysis of DNA FISH as demonstrated by existing microarray technologies. To the best of our knowledge, large-scale DNA FISH has not been demonstrated on single-cell arrays.

The ideal method for preparing a single-cell array for DNA FISH should be simple and inexpensive, so that it can easily be adopted by biologists and medical researchers. The array must also be compatible with FISH, which involves harsh conditions such as repeated washings and elevated temperature. Various methods have been developed to produce single-cell arrays and can be divided into two groups. One relies on use of a passive method of seeding cells on a substrate bearing cell-binding/trapping surface features, such as a flat chemical coating,[10,11] recessed topological structures called microwells,[12–15] or a combination of the two,[16–18] surrounded by a cell-repelling background. This group of methods has the advantage of being relatively easy to perform. In particular, the arrays formed on a flat surface closely resemble conventional FISH samples based on immobilizing cells on a homogeneous surface, so conventional FISH protocols could easily be adapted for the cell arrays without significant modifications. The other group is based on using an active means to form cell patterns.[19–23] Notably, mRNA FISH has been performed on a small array of 100 cells prepared by this strategy.[19] Although enjoying advantages such as independence of cell types and relatively short preparation times, these methods suffer from the need for microfluidic devices, which increase the complexity of this approach and preclude its use by labs lacking the proper expertise.

Here we present a novel method of preparing single-cell arrays for DNA FISH. It is based on chemically micropatterning a flat surface to create an array of cell-adhesive islands and a cell-repelling background, followed by passive seeding of cells. It is simple and inexpensive and allows easy adaptation of conventional FISH protocols. Moreover, the surface chemistry and geometries of the array substrate were specifically selected and designed for FISH. We have used this method to create centimetre-sized single-cell arrays of nonadherent human cells, performed DNA FISH on the arrays, and analyzed the results with a computer program specifically for FISH data analysis.

Methods and materials

Materials

Formamide, formalin, NP-40 surfactant, saline-sodium citrate

(SSC) buffer, HyClone cosmic calf serum, 100× TE (1000 mM Tris HCl and 100 mM ethylenediaminetetraacetic acid) buffer, propidium iodide (PI), and glass slides including 0.17-mm-thick glass coverslips and 1-mm-thick glass microslides were purchased from VWR. Polyvinyl alcohol (PVA, 87–90% hydrolyzed, Mw = 30,000–70,000 Da), octyltrichlorosilane (OTS), 3-aminopropyltriethoxysilane (APTES), and rhodamine-B-isothiocyanate (RITC) were purchased from Sigma-Aldrich. The Sylgard® 184 polydimethyl siloxane (PDMS) kit was purchased from Dow-Corning. ProLong® Gold antifade reagent containing 4',6-diamidino-2-phenylindole (DAPI) and YOYO-1 dye were purchased from Invitrogen. Poly(ethylene glycol) (PEG) silane ([hydroxyl (polyethyleneoxy) propyl] triethoxy silane, Mw = 575–750 Da, 8–12 ethylene glycol units) was purchased from Gelest (Morrisville, PA). K562 and RCH-ACV cell lines were from the American Type Tissue Culture Collection (Rockville, MD) and Deutsche Sammlung von Mikroorganismen und Zellkulturen GmbH (Braunschweig, Germany) respectively. Fetal bovine serum (FBS) was purchased from Atlanta Biologicals (Lawrenceville, GA). FISH probe CEP 3 (D3Z1) SpectrumOrange Probe (locus: 3p11.1-q11.1 alpha satellite DNA) was purchased from Abbott Molecular (Des Plaines, IL). Lambda phage DNA was obtained from New England Biolabs (Ipswich, MA).

Cell culture

K562 cells were cultured in RPMI 1640 medium supplemented with 10% (v/v) cosmic calf serum, 100 units/mL of penicillin, and 100 µg/mL streptomycin at 37°C and 5% CO_2. RCH-ACV cells were cultured in RPMI 1640 medium supplemented with 20% (v/v) FBS, 100 units/mL of penicillin, and 100 µg/mL streptomycin at 37°C and 5% CO_2.

Measurement of cell sizes

Suspended K562 and RCH-ACV cells were roughly spherical in shape. Diameters of 58 K562 cells and 97 RCH-ACV cells were measured under an optical microscope, and the results were used to calculate the average diameters and standard deviations for the two cell types.

Geometrical design of cell arrays

To maximize cell density, we used a hexagonal lattice for the cell-adhesive islands and made the cell-adhesive islands circular because the cells are roughly spherical. To ensure single-cell occupancy, we made the diameter of each island significantly smaller than the average cell diameter. Smaller islands also allowed more precise control of the locations of the cells and are therefore preferable for automated data acquisition and analysis. On the other hand, reducing the island size is expected to lower the adhesion force between the cells and the islands, which must still be strong enough to withstand the series of soaking and rinsing steps in FISH process. For the K562 cells, which were 17.8 µm in average diameter (range 10.1–23.8 µm, standard deviation 2.2 µm), we therefore gave the islands a diameter of 10 µm. For the smaller RCH-ACV cells (average diameter 10.8 µm, range 6.6–15.0 µm, standard deviation 1.6 µm), we gave them a diameter of 5 µm. To ensure separation of the cells from their neighbours in the array while maintaining a relatively high density, we used a centre-to-centre distance of 30 µm for both lattices.

Preparation of PDMS stamps

Central to our surface micropatterning method was microcontact printing,[24,25] which relied on the use of PDMS stamps. We prepared PDMS stamps by casting PDMS prepolymer and curing agent on masters prepared by photolithography.[26] Stamps for the two sizes of adhesive island consisted of arrays on a hexagonal lattice of circular micropillars with diameters of 5 and 10 µm and separated by centre-to-centre distances of 30 µm. The micropillars of all stamps were 8 µm high.

Preparation of slides coated with APTES, OTS, and PEG silane

Glass slides were cleaned with oxygen plasma (PDC-32G plasma cleaner, Harrick Plasma, Ithaca, NY) for 3 min at 350 mTorr and high power level. Slides to be coated with APTES or OTS were placed, with ~100 µL APTES or OTS, in a centrifuge tube in a vacuum desiccator. The desiccator, under vacuum, was placed in an oven at 65°C. After 24 h, the slides were taken out, washed with water, and dried under a stream of nitrogen. The APTES or OTS-coated surfaces were hydrophobic. To prepare glass slides coated with PEG silane, the slides were soaked in the PEG silane 1% (v/wt) in toluene. After 24 h, the slides were washed first with ethanol to remove residual PEG silane and then with water.

Assessing cell adherence to APTES, OTS, and PEG-coated surfaces

A circular hole 1.27 cm in diameter was made in a 3-mm-thick PDMS film. The film was then laid over a slide coated with APTES, OTS, or PEG silane, forming a circular chamber 1.27 cm in diameter, and a 200 µL suspension of live cells in PBS at concentrations of 3.1×10^6, 3.1×10^6, and 0.8×10^6 cells/mL for APTES, OTS, and PEG-coated surfaces respectively was placed in the chamber. The assembly was placed in a Petri dish and then in a cell-culture incubator at 37°C and 5% CO_2. After 1 h, the floating and loosely bound cells were gently washed off, leaving attached cells on the slides.

Preparation of array substrates for cell patterning

The procedure for preparation of array substrates is shown schematically in Fig. 1. (1) A 10% (wt/wt) aqueous solution of PVA, a water-soluble synthetic polymer traditionally used as a surfactant to stabilize oil-in-water emulsions, was spun on a PDMS stamp at 800 rpm for 1 min and then at 1700 rpm for 1 min by means of spin coating. (2) The PVA-coated stamp was placed on an APTES-coated slide. Slight pressure was applied manually to the stamp to ensure full contact between the stamp and the slide. (3) The stamp and slide were placed together on a hot plate set at 100°C for 0.17-mm-thick slides and 150°C for 1-mm-thick slides. (4) The stamp was removed from the slide manually after it spontaneously detached from the slide, typically within 15 sec. (5) The slide was exposed to oxygen plasma for 30 sec at 350 mTorr and medium power level to remove APTES from areas unprotected by PVA. (6) The slide was soaked in PEG silane 1% (v/wt) in toluene for 24 h. (7) The slide was washed first with ethanol, which removed residual PEG silane, and then with water, which removed PVA, leaving an array of APTES islands surrounded by a PEG background on the slide.

Fluorescence staining of APTES islands by RITC and DNA

For RITC staining, the array substrate was soaked in 0.01% (wt/v) RITC in ethanol for 1 h and then washed with copious amounts of ethanol. For DNA staining, 40 µL solution of 2 ng/µL lambda DNA, which was labelled with YOYO-1 dye at

dye-to-base pair ratio of 1/20, in 50 mM MES (2-(N-morpholino) ethanesulfonic acid, pH 5.5) buffer was added on an APTES-island array and covered with a 2-cm-wide coverslip. After 20 min at room temperature, the coverslip was removed, and the array substrate was examined.

Generation of single-cell arrays

A hole-bearing PDMS film like the one described above was placed on an array substrate to form a circular chamber 1.27 cm in diameter, and a 200 µL suspension of live cells in PBS was placed in the chamber. The assembly was placed in a Petri dish and then in a cell-culture incubator at 37°C and 5% CO_2. The dish was briefly tapped manually every 15 min. After incubation, the floating and loosely bound cells were gently washed off, but a thin layer of buffer was left on the surface. The effects of incubation time and cell quantity on the quality of the arrays were studied.

Examination of single-cell arrays

To quantify the quality of the arrays accurately, we repeated each experimental condition (quantity of seeding cells, time of seeding) 3 times. Four micrograph images were taken and analyzed for each sample. Individual islands occupied by a single cell, two cells, and three cells were identified and counted. Individual islands occupied by more than 3 cells were not observed. Cells that were neither located on an island nor adhering to any cell on an island were regarded as being on the background.

Generation and examination of randomly immobilized cells

The same procedure for seeding cells on the APTES-coated surface in section "Assessing cell adherence to APTES, OTS, and PEG-coated surfaces" was used here except that K562 cell suspensions of three different concentrations (0.4×10^6, 0.8×10^6, and 1.6×10^6 cells/mL) were applied to the slides respectively. The slides were then immersed in 4% (v/v) formaldehyde in PBS for 30 min at room temperature and washed with PBS (2 times, 5 min each). 200 µL 20 µg/mL PI was added on each slide and kept for 30 min. Fluorescence micrographs of the immobilized cells were recorded and analyzed with NIS-Elements program. The program allowed identifying regions, in which all pixels were brighter than a threshold, in a micrograph. The threshold was set by the experimenters so that the regions properly represented the cells. The program generated a list of the regions (total number: N_{total}) with area of each region. We believed a region smaller than 30 μm^2 was too small to be a single intact K562 cell. The number of these regions was counted from the list as N_{small}. Since a cell on an edge of a micrograph is partially missing, it was thus not used for analysis. Number of the regions that resided on the edges and were equal to or larger than 30 μm^2 was counted manually as N_{edge}. Number of the regions that appeared to comprise two or more cells, were equal to or larger than 30 μm^2, and did not reside on the edges was manually counted as $N_{cluster}$. With these data collected, number of single isolated cells in the micrograph was calculated as $N_{single} = N_{total} - N_{small} - N_{edge} - N_{cluster}$. For each concentration of the cell suspensions, 6 samples were examined with 2 micrographs per sample being recorded.

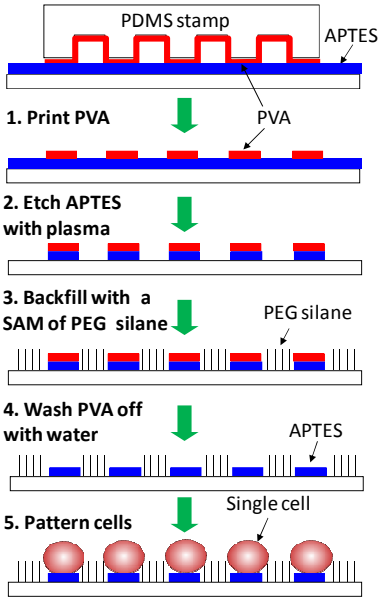

Fig. 1. Schematic of process for fabricating the single-cell array: (1) Polyvinyl alcohol (PVA) dots are printed on a 3-aminopropyltriethoxysilane (APTES)-coated slide. (2) APTES is etched away with oxygen plasma from areas unprotected by PVA dots. (3) The bare glass areas are filled with a self-assembled monolayer (SAM) of cell-repelling poly(ethylene glycol) (PEG) silane. (4) PVA dots are washed away with water to expose the APTES islands. (5) Cells are allowed to adhere to the APTES islands, creating the single-cell array.

FISH

DNA FISH was performed on the K562 cell arrays. FISH probe mixture was prepared by a procedure recommended by the manufacturer of the probe. The FISH protocol recommended by the manufacturer was adopted (with modifications): (1) The slide was immersed in 4% (v/v) formaldehyde in PBS for 24 h at room temperature. (2) The slide was washed twice with PBS, 5 min each. (3) The slide was incubated in acetic acid/methanol (3:1 v:v) for 24 h at room temperature. (4) The slide was dried on a hot plate at 50°C for 3 min. (5) The slide was immersed in prewarmed 73°C denaturation solution (70% (v/v) formamide/2× SSC, pH 7–8) for 5 min. (6) The slide was successively immersed in 70%, 85%, and 100% (v/v) ethanol for 1 min each at room temperature. (7) Excess ethanol was drained from the slide by blotting on a paper towel, and the underside of the slide was wiped. (8) The slide was dried on a hot plate at 50°C for 3 min. (9) Ten µL CEP probe mix was added to the sample area of the slide, the area was covered with a coverslip, and the edges were sealed with rubber cement. (10) The slide was placed in a prewarmed humidified chamber, the chamber was sealed, and the slide was incubated for 24 h at 42°C. (11) The rubber cement seal was removed from the slide, and the slide was immersed in 50% (v/v) formamide/2× SSC at room temperature until the coverslip floated off. (12) The slide was immersed 3 times in 50% (v/v) formamide/2× SSC wash solution at 46°C, 10 min each. (13) The slide was immersed in 2× SSC at 46°C for 10 min. (14) The slide was immersed in 2× SSC/0.1% (wt/v) NP-40 at 46°C for 5 min. (15) The slide was air-dried in darkness at room temperature (for about 25 min). (16) Ten µL of antifade DAPI was applied to the array area and covered with a coverslip atop, and the edges of the coverslip were sealed with nail polish.

Imaging

The optical micrographs were obtained with an inverted Nikon Ti epifluorescence microscope equipped with an Andor iXonEM+ 885 EMCCD camera and an inverted Deltavision deconvolution fluorescence microscope (Applied Precision) equipped with a CoolSNAP HQ CCD camera. The three-dimensional images of fixed nuclei were captured at different stage positions and processed with deconvolution software (SoftWoRx 3.5.0, Applied Precision) for the analysis. Atomic-force microscopy images were obtained with a Veeco Dimension 3000 system at tapping mode in air.

Results and discussion

Preparation of array substrates

We found that an unpatterned self-assembled monolayer (SAM) of APTES (widely used to render a glass surface positively charged as a result of protonation of the primary amines capping the molecules[27,28]) could immobilize a monolayer of nonadherent K562 cells (Fig. S1 in electronic supplementary information (ESI)). Because the surfaces of many types of mammalian cells are negatively charged as a result of presence of sialic acids,[29] electrostatic attraction was likely responsible for the adherence of the K562 cells to the APTES surface. However, surface-grafted PEG terminated with a hydrophobic hydrocarbon chain also allowed adsorption of K562 cells,[30] and because the APTES SAM was hydrophobic, hydrophobic interaction might also have played an important role in immobilizing the cells. Based on the observation that K562 cells did not adhere to a hydrophobic OTS-coated slide (Fig. S1 in ESI), we concluded that electrostatic attraction was responsible for immobilization of the cells on the APTES-coated surface. It is worth noting that polylysine, a positively charged polypeptide, has also been used to coat cell-adhesive islands and wells to generate single-cell arrays of h-TERT-RPE1 (human retinal pigment epithelial) cells and human MOLT 3 T-lymphocytes, respectively.[31,32] PEG silanes with both short and long chains are standard surface-coating materials used to prevent adherence of proteins and cells.[33,34] We tested K562 cells on an unpatterned PEG silane SAM and found no adherence of the cells to the surface (Fig. S1 in ESI). Based on these results, we selected APTES and PEG silane to prepare the cell-adhesive islands and cell-repelling background respectively.

Our method of printing PVA on an APTES-coated surface is similar to that developed by Guan et al. for printing a water-insoluble polymer.[35] Arrays as perfect as that in Fig. 2a were usually obtained throughout the entire stamping area. Atomic-force microscopy characterization of the PVA dots showed that the PVA film is ~98 nm thick at its centre (Fig. 2b), thick enough to block the oxygen plasma etching. Photoresist films patterned by standard photolithography have also been used as masks to block oxygen-plasma etching for patterning of SAMs,[36,37] but the PVA mask is superior because it costs less, does not require expensive cleanroom-based facilities for micropatterning, and can be removed with water rather than organic solvents or harsh etchants. In another method, a photoresist film was coated on a PVA film, then patterned by photolithography, and finally used as a mask for reactive ion etch.[31] The PVA film allowed removal of the photoresist mask with water. It should be noted that all of the above methods used photolithography every time for device fabrication. Although photolithography was also used to prepare the master for generating the PDMS stamps in our method, the master could be used to fabricate many (>50) stamps and a stamp could be used many times (>10) for PVA printing. Our method is thus considerably more cost effective than the photolithography-based methods. To the best of our knowledge, this was the first time that a water-soluble polymer was printed by μCP for use as masks for plasma etching.

Generation of the APTES islands was confirmed by fluorescent staining with RITC, which reacts with the primary amines of APTES. Fig. 2c shows a uniform array of fluorescent islands, which typically covered the entire stamping area, but successful RITC staining did not exclude the possibility that a thin layer of PVA and/or PEG silane was left or formed atop the APTES islands. The layer might allow penetration by RITC, which is a small molecule, but keep APTES inaccessible to large entities such as cells. We therefore used lambda DNA (a macromolecule with a coil diameter of approximately 1.4 μm in water[38]), which is negatively charged and can bind to APTES by electrostatic interaction, to test the accessibility of APTES. We observed binding of fluorescently labelled DNA to the APTES islands as shown in Fig. 2d, proving that the APTES was accessible to macromolecules and therefore probably to cells.

Generation of single-cell arrays

K562, a nonadherent cell line derived from human chronic myeloid leukaemia, was the major model cell line used in our study.[39] Because only single cells located on the APTES islands and separated from their neighbours were useful for DNA FISH analysis, we used single-cell occupancy (SCO), defined as the ratio of the number of cell-adhesive islands occupied by single cells to the total number of the islands within a certain area, as an

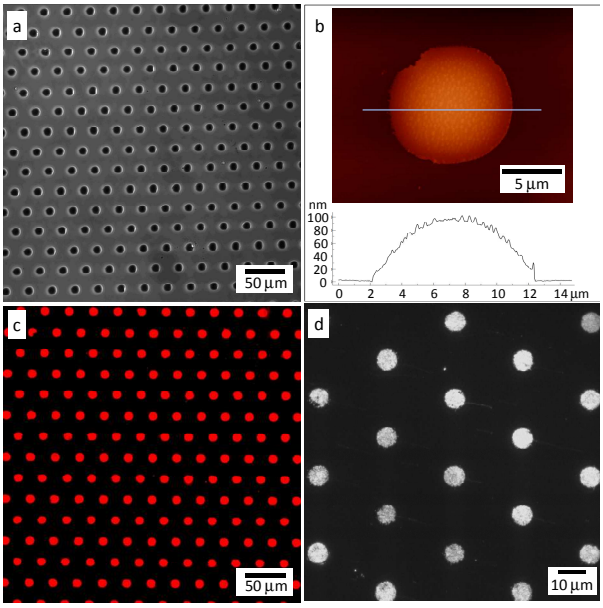

Fig. 2. (a) Phase-contrast micrograph of 10-μm-wide circular PVA dots (black) printed on an APTES-coated glass slide. (b) Height atomic-force microscopy image of a PVA dot on APTES (upper panel) and its line profile (lower panel). Fluorescence micrograph of APTES islands stained with fluorescent rhodamine-B-isothiocyanate (RITC) (c) and YOYO-1–labelled lambda DNA (d).

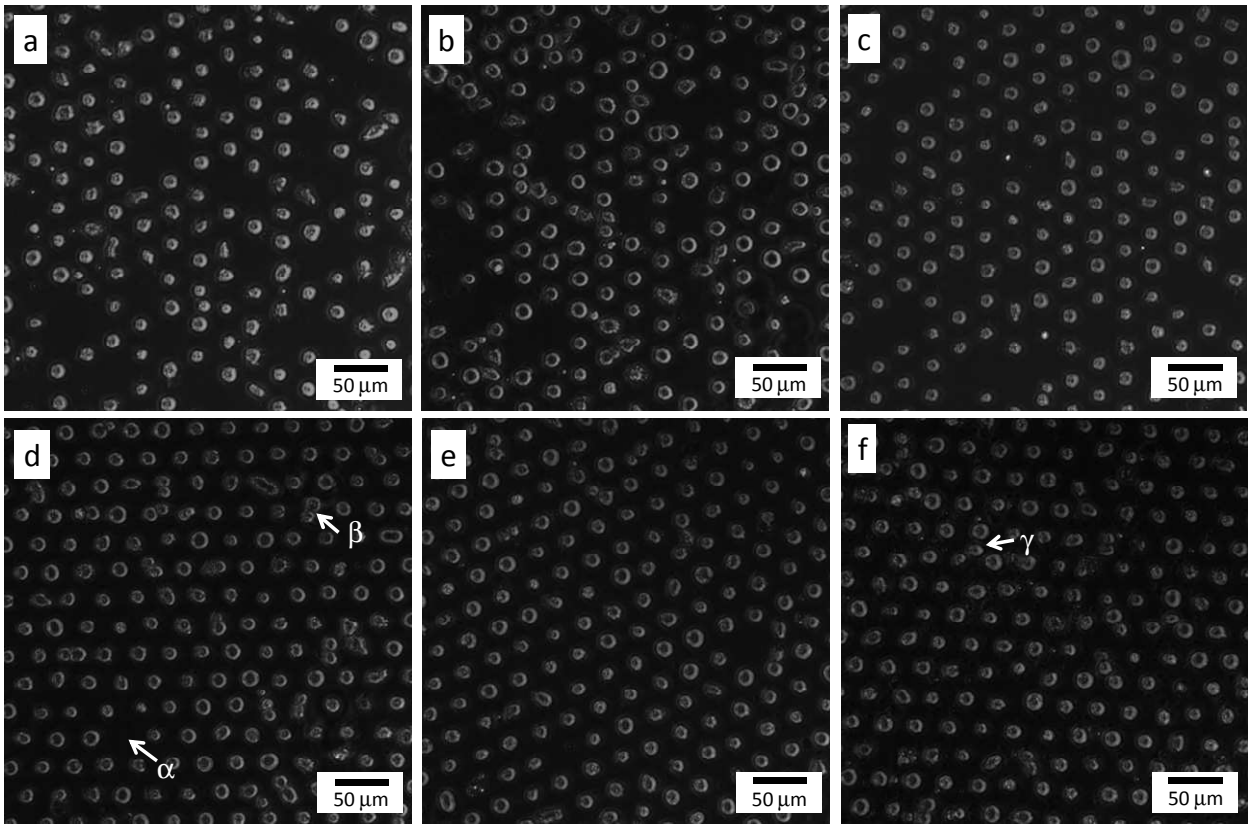

Fig. 3. Phase-contrast micrographs of single-cell arrays formed at cell-seeding times of 15 (a), 30 (b), 45 (c), 60 (d), 90 (e), and 120 (f) min. The seeding cell density (SCD, ratio of number of cells to number of APTES islands) was 2. At 15 min, a cell array formed with a relatively low array occupancy. The array occupancy increased as time elapsed until 60 min. After 60 min, the array occupancy appeared level. Defects, including empty islands, single islands occupied by two cells, and cells on the background are indicated by arrowheads labelled α, β, and γ, respectively.

index of array quality. We hypothesized that SCO was affected by the quantity of cells available and the duration of seeding. Because all cell arrays were produced in chambers with the same geometry, we defined the seeding-cell density (SCD) as the ratio of the number of cells to the number of cell-adhesive islands in the chamber. Three SCDs were used in this study. Since the cell suspension added into a chamber was always 200 µL, SCDs of 0.5, 1, and 2 were equivalent to concentrations of 0.4×10^6, 0.8×10^6, and 1.6×10^6 cells/mL. At each of three SCDs, 0.5, 1, and 2, we used a series of cell-seeding times from 15 to 120 min. Fig. 3 shows representative micrographs of cell arrays prepared at SCD of 2 and seeding times of 15, 30, 60, 90, and 120 min. Clearly single cells were immobilized on the array substrate in the same pattern as the APTES islands in Fig. 2. The cell arrays typically covered the entire 1.27-cm-wide circular areas. We counted the islands occupied by single cells in all cell-array samples, calculated the SCOs, and plotted the SCOs against time at all three SCDs in Fig. 4. These results show that the cell arrays

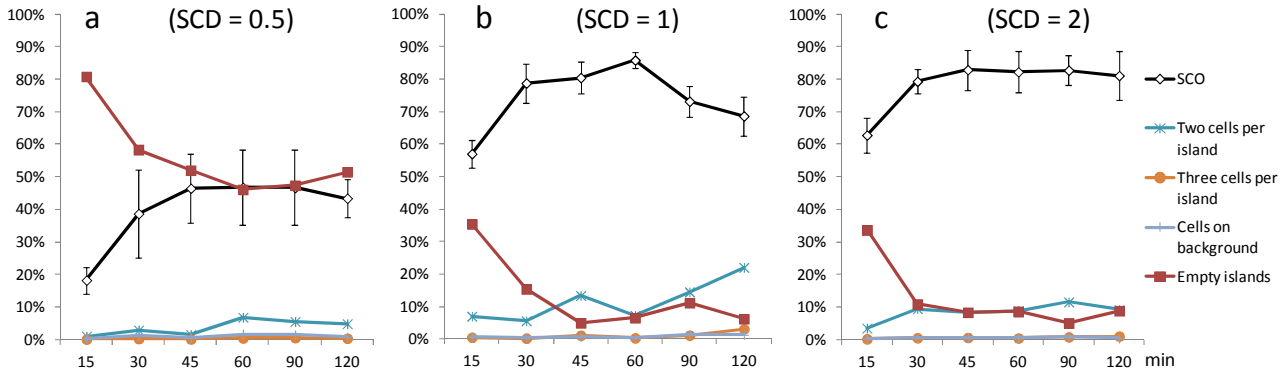

Fig. 4. Dependence of single-cell occupancy (SCO) and densities of four types of array defects (2 cells per island, 3 cells per island, cells on background, and empty islands) on seeding time at SCD of 0.5 (a), 1.0 (b), and 2.0 (c).

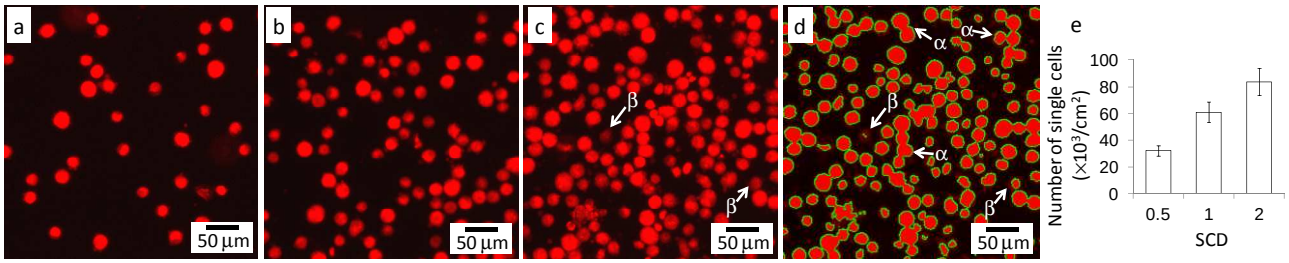

Fig. 5. Fluorescence micrographs of K562 cells immobilized on unpatterned APTES-coated surfaces at SCDs of 0.5 (a), 1 (b), and 2 (c) respectively. Seeding time = 60 min. The cells were stained with propidium iodide. (d) Analysis of micrograph (c) using a computer program for identifying and counting single cells. Green contours are generated by the program to enclose regions in which all pixels were brighter than a threshold. Numbers of single cells were calculated from data extracted from the fluorescence micrographs. Many cells were clustered as exemplified by the three clusters pointed by arrowheads labelled α. Some cells were partially selected as exemplified by the two cells pointed by arrowheads labelled β. (e) Histogram of numbers of single cells per cm^2 at different SCDs.

started to emerge as early as 15 min after the cells were applied at all SCDs. SCOs generally increased from 15 to 60 min and remained level or even decreased thereafter. The highest SCO was 86%, obtained at SCD of 1 and seeding time of 1 h.

Defects were observed in all single-cell arrays, including empty cell-adhesive islands, islands occupied by more than one cell, and cells on the background area, as shown in Fig. 3. The defects can affect analysis of the FISH data by a computer program. For example, cell-adhesive islands occupied by more than two cells can generate FISH signals, but assigning the signals accurately to individual cells is difficult for existing FISH-analysis computer programs.[4] Identification of this type of defect poses a key challenge for developing a computer program specifically for analyzing the FISH array data. To generate a quantitative view of our method and identify optimum conditions for preparing the cell array, we counted islands occupied by two cells, those occupied by three, and cells on the background in all cell-array samples. No islands occupied by more than three cells were observed. The numbers of empty islands were obtained by subtraction of the numbers of occupied islands from the total number of islands. The data are presented in Table S1 in ESI. We defined defect density as ratio of the number of a type of defect to the total number of islands over a certain area and plotted defect densities for all types of defects against seeding time in Fig. 4. Densities of defects, except empty islands, generally increased with time during the initial 60 min. Empty islands displayed the opposite trend. Clearly, the densities of islands occupied by two cells at SCDs of 1 and 2 were higher than those at SCD of 0.5.

An ideal single-cell array for large-scale FISH should have a maximum SCO and minimum defect densities, and short seeding time is desirable. As Fig. 4 shows, we found no experimental conditions satisfying all these requirements. At SCDs of 1 and 2 and seeding time of 60 min, the SCOs and densities of empty islands started to plateau, and densities of other defects were not significantly higher than those under other conditions. We therefore identified these conditions as the optimum for preparing single-cell arrays for FISH. Each of the 1.27-cm-diameter array areas included 162.4×10^3 APTES islands, so at SCO of 86% (SCD = 1, seeding time = 60 min), about 139.7×10^3 islands were occupied by single cells. These cells would be useful for FISH analysis if they retained their positions after FISH.

To quantitatively compare the single-cell array with randomly immobilized cells prepared by the conventional method, we incubated K562 cells on unpatterned APTES-coated surfaces with the same quantities of seeding cells as those at SCDs of 0.5, 1, and 2 for preparing the arrays. The immobilized cells were randomly distributed and the cell density increased with SCD as shown in Figs. 5a, 5b, and 5c. Moreover, the number of cells that touched their neighbours also increased with SCD. NIS-Elements was used to assist identification of isolated single cells in the micrographs as exemplified in Fig. 5d. A threshold fluorescence intensity was manually set. Neighbouring pixels that were brighter than the threshold were grouped as a region, which might consist of a single cell, a cluster of cells, a portion of a cell, or an unknown object. While a high threshold tended to increase the number of clustered cells, a low threshold tended to ignore dim cells and parts of some cells. Either case is undesirable for FISH analysis because over-clustering reduces number of single cells useful for analysis and FISH signals may present in the cellular parts or cells ignored by the program. Fig. 5d shows existence of both cell clusters and partially selected cells, indicating that the above dilemma might be intrinsic to the conventional method. Statistical analyses revealed that the number of single cells rose from 32.1 (±3.9)× 10^3 and 61.0 (±7.5)× 10^3 to 83.6 (±10.2)× 10^3 cells/cm^2 at SCD of 0.5, 1, and 2 respectively (Fig. 5e). Given the fact that the SCO of 86% of our single-cell array is equivalent to 110.3×10^3 cells/cm^2, the array method achieved a higher single-cell density than the

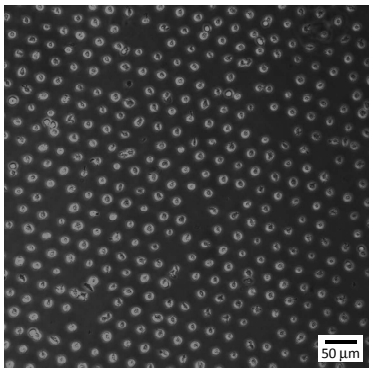

Fig. 6. Phase-contrast micrograph of a single-cell array of RCH-ACV cells.

conventional method. Perhaps more importantly, the highly ordered and well separated fashion of the single-cell array is expected to allow easy and unambiguous data analysis based on the availability of both fluorescence and spatial information of the cells.

In addition to K562 cells, RCH-ACV cells, from a lymphoblastic leukaemia line,[40] were successfully patterned into arrays (Fig. 6) on 5-µm-diameter APTES islands (SCD = 6, seeding time = 60 min). This result indicates that the method is applicable to other cell lines. However, it should be noted that probably only cells with relatively high density of negative surface charges can be patterned by this method.

FISH and analysis

DNA FISH was performed on K562 cell arrays prepared at SCD of 2 and seeding time of 60 min. The harsh conditions typical of DNA FISH—exposure to elevated temperature and repeated soaking and washing—can remove or dislocate patterned cells in a single-cell array. Strengthening the binding between the immobilized cells and the APTES islands would alleviate this potential problem. Formaldehyde is a fixative commonly used in FISH to crosslink proteins with primary amines, and because APTES is terminated with primary amines, we believed that formaldehyde would cause cross-linking of the APTES SAM with proteins on the cell surface. The cell arrays were therefore soaked in formaldehyde solution for 24 h. Fig. 7a shows an array of cell nuclei after the FISH process, revealing that the cell nuclei largely retained their positions. However, the relatively long exposure to formaldehyde might have increased the degree of cross-linking among the nuclear proteins, reducing the accessibility of the genomic DNA to the FISH probes. To avoid this problem, we soaked the cell arrays in acetic acid/methanol for 24 h because acetic acid/methanol soaking can remove nuclear proteins from cells.[41,42]

The FISH result is shown in Fig. 7b; FISH signals are the red dots within the blue areas which are DAPI-stained cell nuclei. Although the FISH signals were found throughout the cell array, only six cells are shown in the figure because the signals are not visible in Fig. 7a due to their small sizes and low brightness. Two or three FISH signals were observed in the cells in Fig. 7b. By analyzing 131 cells in a single-cell array, we found 64.9% of cells contained 2 FISH signals; 19.1% contained 4 signals, 4.6% and 1.5% contained 1 and 3 signals respectively, and 9.9% did not show any signals (Fig. 7c). Note that the targets of the FISH probe are the centromeres of chromosome 3, and a K562 cell contains two chromosome 3s that are apparently normal.[43] We therefore expected a K562 cell to contain 2–4 FISH signals depending on the cell phase, and the FISH result was consistent with this expectation. Although single-cell arrays have been produced by various methods, this study was the first to demonstrate successful performance of DNA FISH over a centimetre-sized array with countable FISH signals, potentially allowing large-scale quantification of genetic features.

Concern may exist regarding the increased time required for preparing the single-cell arrays and performing FISH on the arrays compared to the conventional method. Approximately 53 h was needed to prepare a batch (around 10) of single cells arrays. It should be noted that 48 h of this period of time was used to deposit SAMs on the glass slides and did not require constant attentions. Moreover, the array substrates, once produced, are expected to be storable as commercial glass slides with similar surface coatings. Two extra steps of 24 h each were used to soak the slides bearing the single-cell arrays in the FISH process compared to the protocol recommended by the manufacturer of the FISH probe. Again the total 48 h period did not require constant attention except the starting and ending points of the two steps and multiple slides can be processed simultaneously. We believe optimization of the method can reduce the times for individual steps. Most importantly, we expect the high-throughput data acquisition and analysis enabled by the single-cell arrays would allow an overall significantly shorter time to perform large-scale DNA FISH than the conventional method.

The envisaged high-throughput, large-scale FISH array technology requires automated analysis. To demonstrate its feasibility, we used a computer program called FISH Finder to analyze the single-cell FISH array.[4,44] Although FISH Finder can extract FISH signals from background and count the signals, it cannot obtain accurate signals from clumped cell nuclei. The single-cell array we developed resolves this problem by keeping the cells isolated from their neighbours. Fig. 7d shows the FISH Finder results for Fig. 7b. FISH Finder easily identified both nuclei and FISH signals, demonstrating the feasibility of performing high-throughput, large-scale data acquisition and analysis of DNA FISH on a single-cell array.

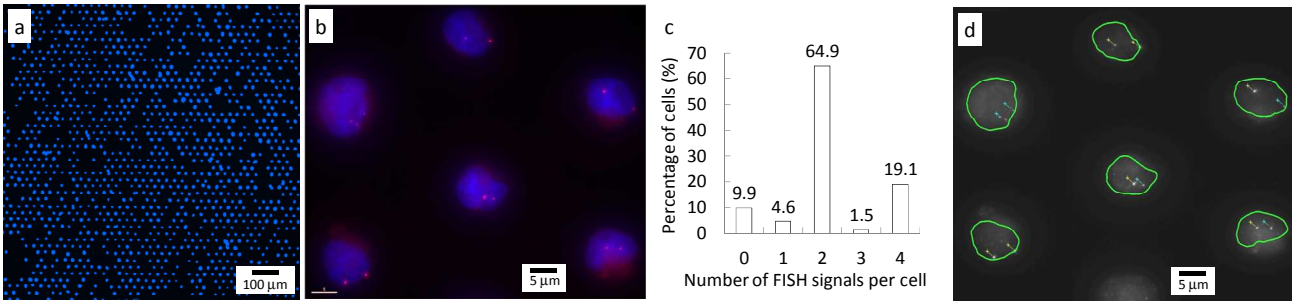

Fig. 7. (a) Fluorescence micrograph of a cell array after the FISH process. The image was taken through a 4',6-diamidino-2-phenylindole (DAPI) filter channel. (b) Fluorescence micrograph of FISH results. FISH signals (red dots) are present in the cell nuclei (blue). (c) Histogram of percentage of cells with different numbers of FISH signals per cell. (d) Analysis of the FISH image (b) by the FISH Finder program. Cell nuclei and FISH signals were identified; contours of the nuclei were generated, and FISH signals are indicated by line segments.

Conclusions

We have developed a novel sample-preparation method for DNA FISH. The method allows creation of centimetre-sized arrays of single cells of nonadherent human leukemic cell lines. It is simple and inexpensive and can therefore potentially be adopted by biologists and medical researchers. DNA FISH has been successfully performed on the single-cell arrays, and the results are analyzable by a computer program, indicating that this method holds potential for realizing high-throughput, large-scale data acquisition and analysis of DNA FISH.

Acknowledgements

We thank Lei Jiang of the Department of Chemical and Biomedical Engineering, Florida State University (FSU), for performing preliminary studies on cell patterning; Anne B. Thistle of the Department of Biological Science, FSU, for editing the manuscript; Dr. Joan Hare at the Institute of Molecular Biophysics, FSU, for assisting with cell culture; Dr. Daniel Gallego Perez of the Department of Biomedical Engineering at The Ohio State University for preparing masters for PDMS casting; and Drs. Bill Chang and Brian Druker of Oregon Health Sciences Center (Portland, OR) for providing RCH-ACV cells. This work was supported by FSU Research Foundation GAP award and Florida Department of Health Bankhead-Coley Cancer Research Program Technology Transfer Feasibility award 1BF03-43278 to JG, and National Institute for General Medical Sciences grant PO1 GM085354 to DMG.

Notes and references

[a] *Department of Chemical and Biomedical Engineering, FAMU-FSU College of Engineering, Florida State University, 2525 Pottsdamer Street, Tallahassee, Florida 32310-2870, USA. E-mail: guan@eng.fsu.edu*
[b] *Department of Biological Science, Florida State University, Tallahassee, Florida 32306-4295, USA*
[c] *Department of Chemistry and Biochemistry, Florida State University, Tallahassee, Florida 32306-4390, USA*
[d] *Integrative NanoScience Institute, Florida State University, Tallahassee, Florida 32306-4370, USA*
† Electronic Supplementary Information (ESI) available: [details of any supplementary information available should be included here]. See DOI: 10.1039/b000000x/

1. J. D. Wolff and S. Schwartz, in *The Principles of Clinical Cytogenetics*, 2nd Edition, Ed. S. L. Gersen and M. B. Keagle, Humana Press, Totowa, NJ, 2004, pp. 455–489.
2. D. G. Hicks and R. R. Tubbs, *Hum Pathol.*, 2005, **36**, 250–261.
3. S. F. Paternoster, S. R. Brockman, R. F. McClure, E. D. Remstein, P. J. Kurtin, and D. W. Dewald, *Am. J. Pathol.*, 2002, **160,** 1967–1972.
4. J. W. Shirley, S. Ty, S. Takebayashi, X. Liu, and D. M. Gilbert, *Bioinformatics*, 2011, **27,** 933–938.
5. R. A. Walker, J. M. Bartlett, M. Dowsett, I. O. Ellis, A. M. Hanby, B. Jasani, K. Miller, and S. E. Pinder, *J. Clin. Pathol.*, 2008, **61**, 818–824.
6. S. Kozubek, E. Lukásová, P. Jirsová, I. Koutná, M. Kozubek, A. Ganová, E. Bártová, M. Falk, and R. Paseková, *Chromosoma*, 2002, **111**, 321–331.
7. H. Knecht, B. Sawan, D. Lichtensztejn, B. Lemieux, R. J. Wellinger, and S. Mai, *Leukemia*, 2009, **23**, 565–573.
8. L. M. Merlo, J. W. Pepper, B. J. Reid, and C. C. Maley, *Nat. Rev. Cancer*, 2006, **6**, 924–935.
9. M. Gerlinger, A. J. Rowan, S. Horswell, J. Larkin, D. Endesfelder, E. Gronroos, P. Martinez, M. Matthews, A. Stewart, P. Tarpey, I. Varela, B. Phillimore, S. Begum, N. Q. McDonald, A. Butler, D. Jones, K. Raine, C. Latimer, C. R. Santos, M. Nohadani, A. C. Eklund, B. Spencer-Dene, G. Clark, L. Pickering, G. Stamp, M. Gore, Z. Szallasi, J. Downward, P. A. Futreal, and C. Swanton, *N. Engl. J. Med.*, 2012, **366**, 883–892.
10. C. S. Chen, M. Mrksich, S. Huang, G. M. Whitesides, and D. E. Ingber, *Science*, 1997, **276**, 1425–1428.
11. J. Nakanishi, Y. Kikuchi, T. Takarada, H. Nakayama, K. Yamaguchi, and M. Maeda, *J. Am. Chem. Soc.*, 2004, **126**, 16314–16315.
12. J. R. Rettig and A. Folch, *Anal. Chem.*, 2005, **77**, 5628–5634.
13. D. K. Wood, D. M. Weingeist, S. N. Bhatia, and B. P. Engelward, *Proc. Natl. Acad. Sci. USA*, 2010, **107**, 10008–11003.
14. S. Yamamura, H. Kishi, Y. Tokimitsu, S. Kondo, R. Honda, S. R. Rao, M. Omori, E. Tamiya, and A. Muraguchi, *Anal. Chem.*, 2005, **77**, 8050–8056.
15. A. Folch, B. H. Jo, O. Hurtado, D. J. Beebe, and M. Toner, *J. Biomed. Mater. Res.*, 2000, **52**, 346–353.
16. A. Tourovskaia, T. Barber, B. T. Wickes, D. Hirdes, B. Grin, D. G. Castner, K. E. Healy, and A. Folch, *Langmuir*, 2003, **19**, 4754–4764.
17. K. Leong, A. K. Boardman, H. Ma, and A. J. Jen, *Langmuir*, 2009, **25**, 4615–4620.
18. H. Kim, R. E. Cohen, P. T. Hammond, and D. J. Irvine, *Adv. Funct. Mater*., 2006, **16**, 1313–1323.
19. T. Matsunaga, M. Hosokawa, A. Arakaki, T. Taguchi, T. Mori, T. Tanaka, and H. Takeyama, *Anal. Chem.*, 2008, **80**, 5139–5145.
20. N. Ferrell, D. Gallego-Perez, N. Higuita-Castro, R. T. Butler, R. K. Reen, K. J. Gooch, and D. J. Hansford, *Anal. Chem.*, 2010, **82**, 2380–2386.
21. M. Hosokawa, A. Arakaki, M. Takahashi, T. Mori, H. Takeyama, and T. Matsunaga, *Anal. Chem.*, 2009, **81**, 5308-5313.
22. J. Y. Park, M. Morgan, A. N. Sachs, J. Samorezov, R. Teller, Y. Shen, K. J. Pienta, and S. Takayama, *Microfluid Nanofluidics*, 2010, **8**, 263–268.
23. D. Di Carlo, N. Aghdam, and L. P. Lee, *Anal. Chem.*, 2006, **78**, 4925–4930.
24. J. L. Wilbur, A. Kumar, H. A. Biebuyck, E. Kim, and G. M. Whitesides, *Nanotechnology*, 1996, **7**, 452─457.
25. T. Kaufmann and B. J. Ravoo, *Polym. Chem.*, 2010, **1**, 371─387.
26. Y. Xia and G. M. Whitesides, *Annu. Rev. Mater. Sci.*, 1999, **23**, 153–a84.
27. Z. Liu, Z. Li, H. Zhou, G. Wei, Y. Song, and L. Wang, *J. Microsc.*, 2005, **218**, 233–239.
28. Z. Tang, Y. Wang, and N. A. Kotov, *Langmuir*, 2002, **18**, 7035–7040.
29. E. I. Finkelstein, P. H. Chao, C. T. Hung, and J. C. Bulinski, *Cell Motil. Cytoskeleton*, 2007, **64**, 833–846.
30. K. Kato, K. Umezawa, D. P. Funeriu, M. Miyake, J. Miyake, and T. Nagamune, *Biotechniques*, 2003 **35**, 1014–1018, 1020–1021.
31. L. Wang, L. Lei, X. F. Ni, J. Shi, and Y. Chen, *Microelectronic Engineering*, 2009, **86**, 1462–1464.
32. A. Revzin, K. Sekine, A. Sin, R. G. Tompkins, and M. Toner, *Lab Chip*, 2005, **5**, 30–37.
33. S. Sharma, R. W. Johnson, and T. A. Desai, *Biosensors Bioelectronics*, 2004, **20**, 227–239.
34. S. Jo and K. Park, *Biomaterials*, 2000, **21**, 605–616.
35. J. Guan, A. Chakrapani, and D. J. Hansford, *Chem. Mater.*, 2005, 17, 6227–6229.
36. B. Kannan, R. P. Kulkarni, S. Satyanarayana, K. Castelino, A. Majumdar, *J. Vac. Sci. Technol. B*, 2005, **23**, 1364-1370.
37. K. Kuribayashi, Y. Tsuda, H. Nakamura, and S. Takeuchi, *Sensors Actuators B Chem.*, 2010, **149**, 177–183.
38. D. E. Smith, T. T. Perkins, and S. Chu, *Macromolecules*, 1996, **29**, 1372–1373.
39. E. Klein, H. Ben-Bassat, H. Neumann, P. Ralph, J. Zeuthen, A. Polliack, and F. Vánky, *Int. J. Cancer*, 1976, **18**, 421–431.
40. I. Jack, R. Seshadri, M. Garson, P. Michael, D. Callen, H. Zola, and A. Morley, *Cancer Genet. Cytogenet*., 1986, **19**, 261–269.
41. A. Sivak and S. R. Wolman, *Histochemistry*, 1974, **42**, 345–349.
42. M. Rønne, O. Andersen, and M/ Erlandsen, *Hereditas*, 1979, **90**, 195–201.
43. S. M. Gribble, I. Roberts, C. Grace, K. M. Andrews, A. R. Green, and E. P. Nacheva, *Cancer Genet. Cytogenet.*, 2000, **118**, 1–8.

44. http://code.google.com/p/fishfinder/downloads/list. Accessed on April 16, 2012.